water

MDPI

Article

Spatial Distribution, Migration, and Ecological Risk of Cd in Sediments and Soils Surrounding Sulfide Mines—A Case Study of the Dabaoshan Mine of Guangdong, China

Weikang Sheng [1], Qingye Hou [1,*], Zhongfang Yang [1] and Tao Yu [2]

[1] School of Earth Science and Resources, China University of Geosciences, Beijing 100083, China; shengwk95@163.com (W.S.); yangzf@cugb.edu.cn (Z.Y.)
[2] School of Science, China University of Geosciences, Beijing 100083, China; yutao@cugb.edu.cn
* Correspondence: qingyehou@cugb.edu.cn

Abstract: Acid mine drainage (AMD) resulting from metal sulfide mining activities can lead to contamination by potentially toxic elements (PTEs) primarily concentrated around the mining area and gradually spreading outward. However, ecological risks do not correspond directly to PTE concentrations, making it challenging to effectively manage the mining environment and accurately prevent potential ecological impacts. In this paper, we analyzed Cd levels in sediments, soils, and corresponding rice grains sampled from four villages near Dabaoshan Mine of Guangdong, China, in 2017. Our results reveal that Cd is the most prominent pollutant element, exhibiting significant enrichment and spatial heterogeneity in both soil and sediments and higher accumulation levels in rice grains compared to other PTEs. Cd concentrations in soil decrease from the tailings pond to the river terrace, with a slight increase after Taiping River joins and flows into the alluvial plain. However, the concentrations in sediments show the opposite trend. The bioconcentration factor (BCF) for Cd in agricultural soil from the river terrace is lower than that from the alluvial plain and the degree of exceeding the maximum permit level (MPL) of Cd in rice grains increases along the river. Mineral transformation and topography are important factors in controlling the geochemical behavior of PTEs. Remediation efforts alter the physicochemical properties of the river, resulting in the release of PTEs during schwertmannite transformation followed by their adsorption by clay minerals. Furthermore, the random forest (RF) analysis highlights that the bioavailability and potential ecological risk of Cd in soils are governed by the occurrence form of Cd in different topographies, mainly controlled by TFe_2O_3, Mn, and CaO in the river terrace and CaO, Al_2O_3/SiO_2, and Mn in the alluvial plain. Therefore, considering the impact of topography on mineral compositions, physicochemical properties, and occurrence form of PTEs in soil and sediments is essential for assessing ecological risk in mining areas.

Keywords: PTEs; sulfide mines; soils; ecological risk; topography

Citation: Sheng, W.; Hou, Q.; Yang, Z.; Yu, T. Spatial Distribution, Migration, and Ecological Risk of Cd in Sediments and Soils Surrounding Sulfide Mines—A Case Study of the Dabaoshan Mine of Guangdong, China. *Water* **2023**, *15*, 2223. https://doi.org/10.3390/w15122223

Academic Editors: Ruiping Liu and Youning Xu

Received: 9 April 2023
Revised: 7 June 2023
Accepted: 11 June 2023
Published: 13 June 2023

1. Introduction

Mining and smelting of metal sulfides result in significant contamination by potentially toxic elements (PTEs) in the surrounding environment, with characteristics of high concentrations of PTEs, multiple contaminants, and large areas with significant ecological risk [1,2]. Soils in mining areas have been contaminated with PTEs globally, posing a major environmental issue in terms of agricultural soil and crop contamination near mining areas [3–7]. Even after mining activities have ceased, PTEs from tailings still continue to be released into the surrounding soil, streams, and groundwater over long periods of time through erosion, weathering, and leaching processes [3].

Dabaoshan Mine is one of China's major large−scale polymetallic sulfide mines [8]. Exploitation of mineral resources has produced a large quantity of tailings containing sulfide minerals. These tailings are continuously oxidized to form acid mine drainage

(AMD) rich in PTEs [9,10]. A large area surrounding the mine has been impacted, posing a threat to the health of local residents [11,12]. The water and soil in 83 villages around Dabaoshan Mine have become contaminated with PTEs, resulting in severe health issues such as cardiovascular, kidney, nervous, blood, and skeletal diseases [13,14], and even esophageal cancer, liver cancer, and other cancers [15,16]. To avoid further contamination, mining activities were halted in 2016. In addition, in response to government policies, mining companies have conducted a series of restoration efforts for AMD treatment, including building mud impoundments to restrict the movement of waste and soil [17], constructing sewage treatment plants [18], and adding lime to the rivers near the mine [19].

PTEs can enter the human body via various exposure pathways from contaminated soil, leading to adverse health effects [20]. Although PTE contamination is primarily concentrated around the mining area and gradually spreads outward, extensive research has demonstrated that the areas with the highest human health risks do not align with the areas exhibiting the highest PTE concentrations in soil [15,21–25]. In the Dabaoshan Mine area, concentrations of PTEs in soils and suspended particles gradually decrease as distance increases from the headwaters of the river [22,23]. Furthermore, PTEs are characterized by high potential bioavailability owing to the high non−residual fractions of PTEs in the sediments and soil [24], and the average concentrations of Cd and Pb in rice grains grown near the mining area exceed the maximum permit levels (MPLs) [25]. Shangba Village is the highest risk area, with Cd being the main pollutant contributing to human health risks, while the risks near the tailings area are within acceptable ranges according to human health risk assessments [21,24]. Areas farther away from the mining area exhibit higher toxicity and greater ecological risks, indicating no obvious correspondence between PTEs in soil and crops, and posing challenges for effective pollution control and risk prevention in mining areas. In addition, the distribution and migration of PTEs around the Dabaoshan Mine after restoration efforts have been rarely studied. Therefore, the objectives of this study were to (1) investigate the characteristics, spatial distributions, and migration of Cd in the environment surrounding the mine, and (2) identify the key factors governing the spatial distributions and bioavailability of Cd.

2. Materials and Methods

2.1. Study Area

Dabaoshan Mine is the largest mine in southern China, and is located in Shaoguan City, Guangdong Province, China (24°31′37″ N, 113°42′49″ E) [8,26]. The Dabaoshan Mine spreads from north to south, with higher elevations in the north (800–1200 m) and lower elevations in the south, including low hills and alluvial plains [27]. The region has a subtropical monsoon climate, with an average annual temperature of 20.3 °C and an average annual precipitation of 1782 mm [28]. Dabaoshan Mine is a well−known large−scale multi−metal sulfide mine with low−temperature mineralization. The main mineralization includes limonite in the upper part, copper−sulfur ores in the middle part, and lead−zinc ores in the lower part, along with non−ferrous metals such as tungsten, bismuth, molybdenum, gold, and silver [29,30].

Since the 1970s, large−scale mining activities have been carried out in the area, resulting in the generation of large amounts of AMD from the waste stacking, ore beneficiation, and washing processes [31]. AMD is discharged from the water outlets of the Tielong and Caoduikeng tailings ponds and flows into the Hengshi and Fanshui Rivers, which converge 1.6 km north of Liangqiao Village before entering the mainstream Hengshi River. The river flows through several villages, including Liangqiao Village (LQ, ~5 km), Tangxin Village (TX, ~9 km), Yanghe Village (YH, ~12 km), and Shangba Village (SB, ~15 km), before it joins the Taiping River, which is not directly affected by mining activities. Shangba Village is known as an endemic cancer village due to its high mortality rate [25]. For this study, we defined the LQ–SB section of the Hengshi River as the upstream area of the Hengshi River. The LQ–TX area has mainly hills and terraces accompanied by high river flow velocity due to a drop in elevation and a narrow valley, while the YH–SB area has mainly alluvial plains, where the riverbed gradually widens and the slope is very gentle [32]. The geological map is shown in Figure S1. Granite outcrops are present and the surface rocks are highly weathered. The study area is covered with quaternary alluvium along Hengshi River and the predominant soil type is laterite [13].

2.2. Sampling

The sampling sites are shown in Figure 1. Sampling was carried out in July 2017 during the rainy season. Six natural forest soil samples were collected in the upstream area of the Hengshi River, including one from TX, two from YH, and three from SB. The sampling depth was 0–20 cm and the sampling density was 4 points/km^2. Four to six subsamples were collected according to the "S" or "X" sampling method. After removing roots and other debris, they were thoroughly mixed and divided into four parts with 1.0–1.5 kg per subsample, which were then placed in sample bags. After drying in a cool place and removing debris, the samples were smashed with a rubber hammer, ground, and sieved through a 10−mesh nylon sieve, and mixed well; each sample weighed >100 g. The samples were then placed in clean polyethylene bags and sent to the laboratory for analysis.

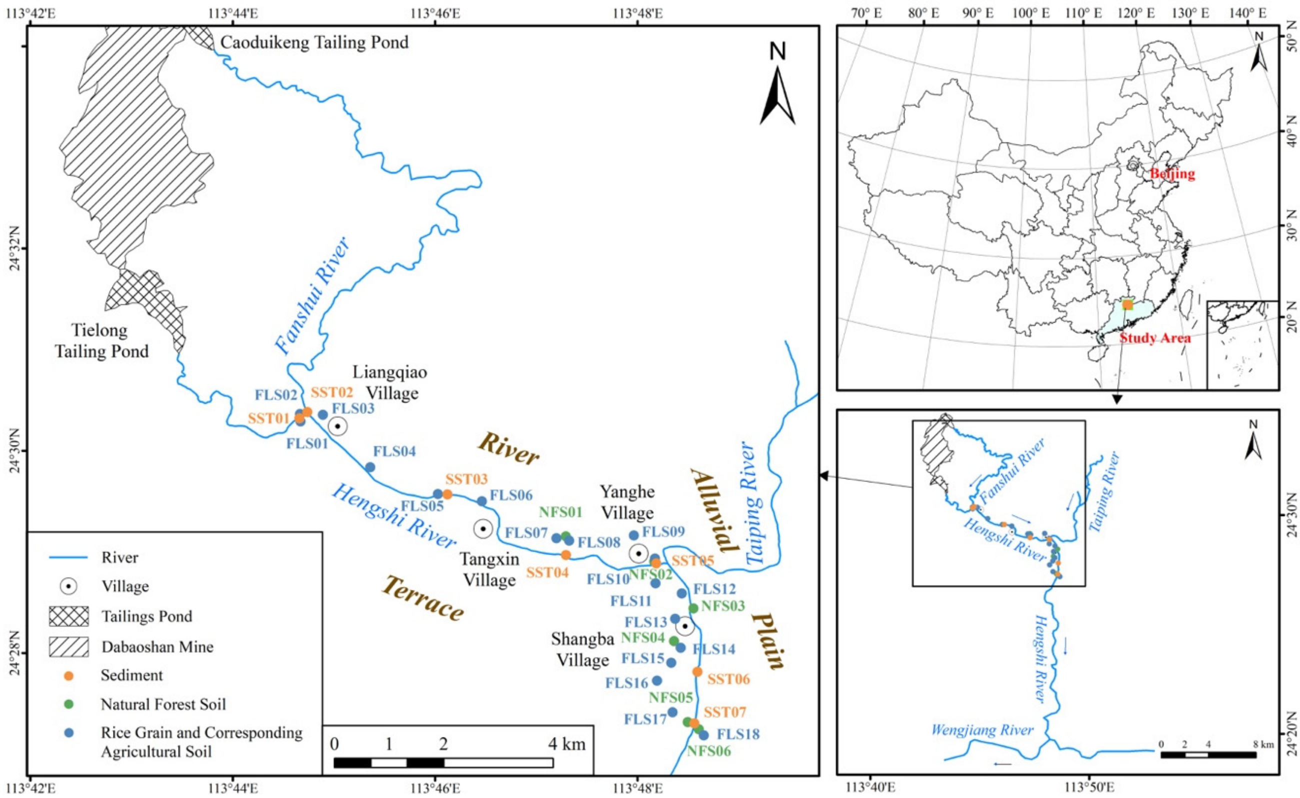

Figure 1. Sampling sites from the upper Hengshi River through the Dabaoshan Mine.

During the rice harvesting period, 18 rice grains and corresponding agricultural soil samples were collected, including 4 from LQ, 4 from TX, 5 from YH, and 5 from SB. Between 3 and 5 soil subsamples were collected at each sampling point and 5–20 plants were collected at each subsample point. The soil and plant subsamples were then mixed into composite samples. The whole rice plant was pulled out of the ground and the ears of rice were cut and placed in clean mesh bags. The root soil was shaken into a clean cotton bag. The ears of rice were air dried in a cool, ventilated, clean, and dust−free place. The panicle was then threshed, removing impurities and husks, ground with an agate mortar to 60 mesh (<0.25 mm), mixed well, and used for further chemical analysis. Plant residues, such as straw and other non−soil components, were removed from the soil samples, and then the samples were air dried. The soil was regularly turned over and beaten during this process. All soil components were sieved through a 10−mesh nylon sieve and mixed well for further chemical analysis.

Seven sediment samples were collected from the Hengshi River. During the collection process, sand was avoided as much as possible, and surface sediments were collected from the 0–5 cm horizon, sealed in polyethylene plastic bags, and numbered. The pH of the river water at the sampling sites was measured and recorded with a handheld pH meter. After air drying, the river sediment samples were sieved through a 10−mesh nylon sieve and ground with a pollution−free ball mill to 200 mesh for analysis.

2.3. Chemical Analysis

Sample analysis was conducted by the Hefei Mineral Resources Supervision and Testing Center, the Ministry of Land and Resources, People's Republic of China. The oxides content was measured directly by wavelength dispersive X−ray fluorescence spectrometry (PANALITICA AXIOS PW4400, Almelo, The Netherlands). Soil samples were dissolved using a mixed acid solution (5 mL HCl, 3 mL HNO_3, 7 mL HF, and 0.25 mL $HClO_4$) and then the samples were dissolved using aqua regia and made up to a volume of 25 mL using high−purity water. Soil samples weighing 5 g were extracted with 50 mL of 0.01 M $CaCl_2$ solution. After centrifugation for 10 min, the supernatant was filtered. Rice grains were washed with deionized water, dried at 105 °C for 5 min, and dried at 70 °C to a constant weight. The plant samples were ground using a stainless−steel grinder and then dissolved using a mixed acid solution (HNO_3:$HClO_4$ = 4:1) until a transparent and clear solution was obtained. Concentrations of Cd, Pb, and Zn in the above solutions were determined using inductively coupled plasma mass spectrometry (ICP−MS) (X−SERIES II, Thermo Fisher Scientific, Waltham, MA, USA) [33]. For soil pH measurement, 10 g of an air−dried soil sample passed through a 2 mm sieve was weighed precisely to 0.01 g and added to a 50 mL high−form beaker. Then, 25 mL of decarbonated water was added (sample to liquid ratio 1:2.5) and the mixture was stirred for 1 min to disperse the sample particles. After standing for 30 min, the soil pH was measured. The cation exchange capacity (CEC) was measured using the $BaCl_2-H_2SO_4$ method. Soil organic matter (SOM) was measured by wet oxidation in an acid dichromate solution, followed by back titration of the remaining dichromate using a ferrous ammonium sulfate standard solution. National standard materials, GBW07405/GBW07458, GBW07304a, and GBW10010 were used to control the data accuracy for soil, sediment, and rice, respectively, and coded samples were added to control the precision of the data. The detailed quality control analysis of data is shown in Supporting Information, and all analytical data met the quality requirements.

2.4. Data Analysis

Basic descriptive statistics were derived to summarize the concentrations of major elements and Cd, Pb, and Zn in the study area. Descriptive statistics and Pearson correlations were analyzed using SPSS 26 (IBM SPSS Statistics). Pearson correlation analysis estimates the linear relationship between two variables. The analysis renders correlation coefficients ranging from −1 to 1, where −1 indicates a perfect negative linear relationship, 0 indicates no correlation, and 1 indicates a perfect positive linear relationship.

Linear regression fit analysis was performed using Origin 2020 (Origin lab Corporation). The cumulative probability distributions were fitted by a logistic function as follows:

$$y = 1/(1 + \exp((a - x)/b)$$

where y is the probability of a given value of x, and a and b are constants.

Random forest analysis was performed using R software (version 4.2.2). Random forest (RF) is a machine learning algorithm that can be used to assess the relative importance of independent variables on a dependent variable [34]. As part of the bootstrap resampling procedure, n samples were randomly selected from the training set to construct decision trees. Meanwhile, a random selection of k (k $\leq$ total number of features) candidate features was performed, and the optimal attribute was selected as the split node [35].

Geographical distribution maps were generated using ESRI−ArcGIS geospatial software (version 10.8).

3. Results

3.1. Concentrations of PTEs in Soils and Sediments

Cd, Pb, and Zn concentrations in natural forest soils, agricultural soils, and sediments in the upper Hengshi River are shown in Figure 2. The corresponding oxides and physicochemical properties are shown in Tables S3–S5. The average concentrations of Cd, Pb, and Zn in sediments are 10.31 mg/kg, 455.01 mg/kg, and 1943.97 mg/kg, respectively. The average concentrations of Cd, Pb, and Zn in natural forest soils are 0.73 mg/kg, 293.13 mg/kg, and 241.90 mg/kg, respectively. The average concentrations of Cd, Pb, and Zn in agricultural soils are 0.50 mg/kg, 96.42 mg/kg, and 179.99 mg/kg, respectively. Using the risk screening values (RSVs) and risk intervention values (RIVs) for Cd, Pb, and Zn shown in Table S1 as standards [36], 67% and 53% of the natural forest soils and agricultural soils exceed the Cd risk screening values (RSVs), respectively. A total of 17% of the natural forest soils exceed the Pb risk intervention values (RIVs), while 33% of the natural forest soils exceed the RSV of Pb. A total of 43% of the agricultural soils exceed the RSV of Pb, and 33% and 47% of the natural forest soils and agricultural soils exceed the RSV of Zn, respectively. Cd is the most serious pollutant in the soils around the Dabaoshan Mine, followed by Pb and Zn. Compared with natural forest soils, the degree of PTE pollution in agricultural soils is lower.

The potential ecological risks of PTEs in sediments were assessed using the threshold effect level (TEL) and probable effect level (PEL) recommended by Sediment Quality Guidelines (SQGs) [37]. When PTEs concentrations are below the TEL, they are considered to pose no or low ecological risk. PTEs concentrations between the TEL and PEL indicate a moderate ecological risk, while concentrations surpassing the PEL indicate a high ecological risk. TELs and PELs for Cd, Pb, and Zn are given in Table S2. Concentrations of Cd, Pb, and Zn in sediments of the upper Hengshi River (Figure 2) are higher than their PELs, indicating a high ecological risk with potential toxic effects on aquatic organisms.

Spatial variations in PTEs concentrations in soils and sediments are shown in Figure 3. Contrary to previous studies, the concentrations of PTEs do not exhibit a consistent decrease [22,23]. Concentrations of Cd, Pb, and Zn in agricultural soils gradually decrease from 1.08 to 0.19 mg/kg from LQ near the mining area to TX, then show a significant positive peak near YH and decrease near SB. Natural forest soils show an overall trend of gradually increasing near TX, then sharply decreasing near YH. Concentrations of Cd, Pb, and Zn in sediments increase from 5.29 to 20.22 mg/kg from LQ to TX, then sharply decrease near YH and gradually increase again near SB.

3.2. Concentrations of PTEs in Rice Grains

Cd concentrations in rice grains in the upper Hengshi River range from 0.014 mg/kg to 2.69 mg/kg with an average value of 1.03 mg/kg, with 95.24% exceeding maximum permit levels (MPLs) (0.20 mg/kg) for rice grains [38]. Concentrations of Pb and Zn in rice grains range from 0.02 to 0.39 mg/kg, and from 15.6 to 23.9 mg/kg, with average values of 0.12 mg/kg and 18.99 mg/kg, respectively. There are no rice grain samples in which concentrations of Pb and Zn exceed MPLs (Table 1). The degree of exceeding the MPL of Cd in rice grains from river terrain ranges from −93% to 290%, with a median value 238%. The degree of exceeding the MPL of Cd in rice grains from alluvial plains ranges from 258% to 1245%, with a median value 573%.

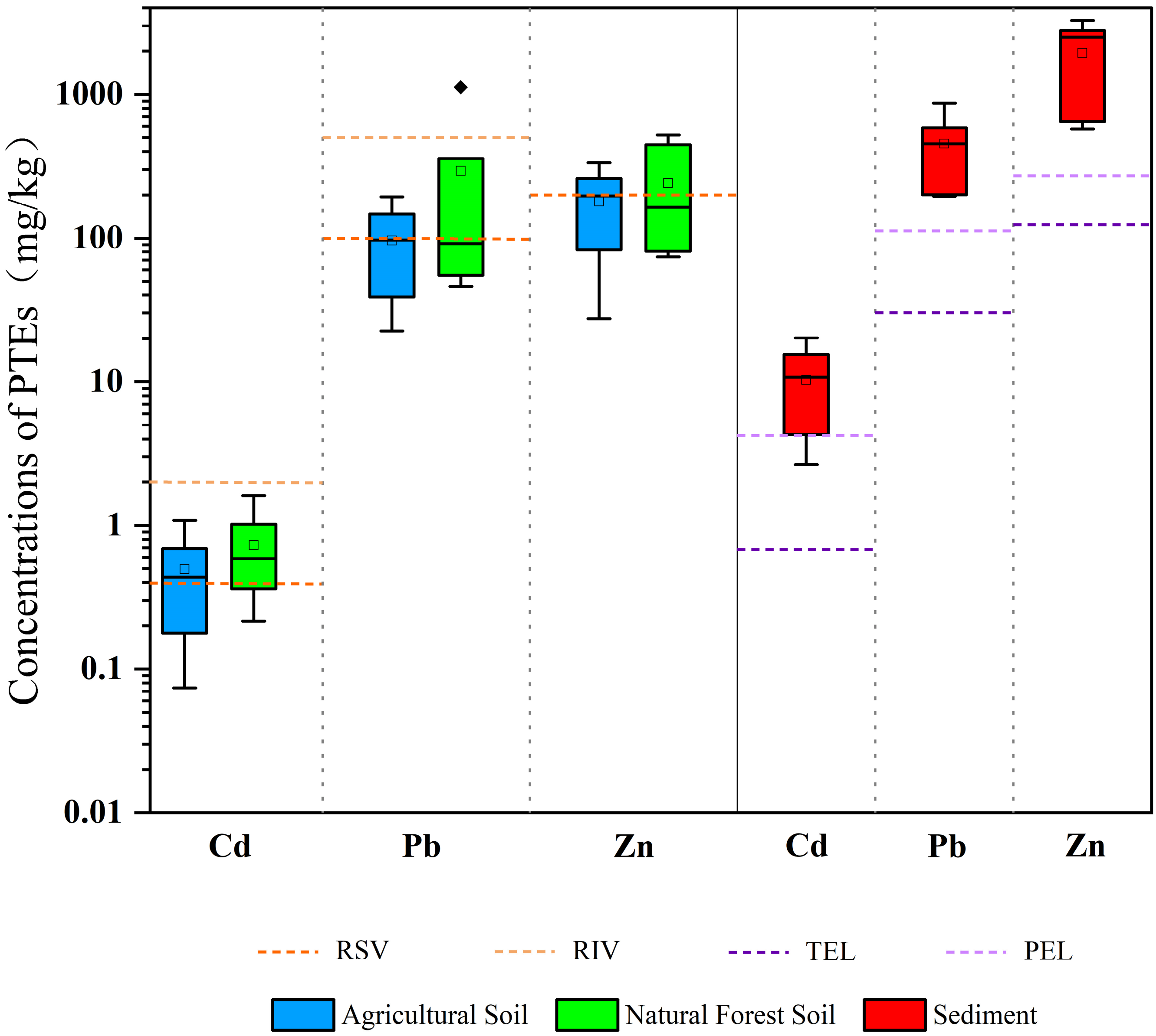

Figure 2. The boxplots for the concentrations of Cd, Pb, and Zn in agricultural soils, natural forest soils, and sediments in the study area (RSV: risk screening value, RIV: risk intervention value, TEL: threshold effect level, PEL: probable effect level).

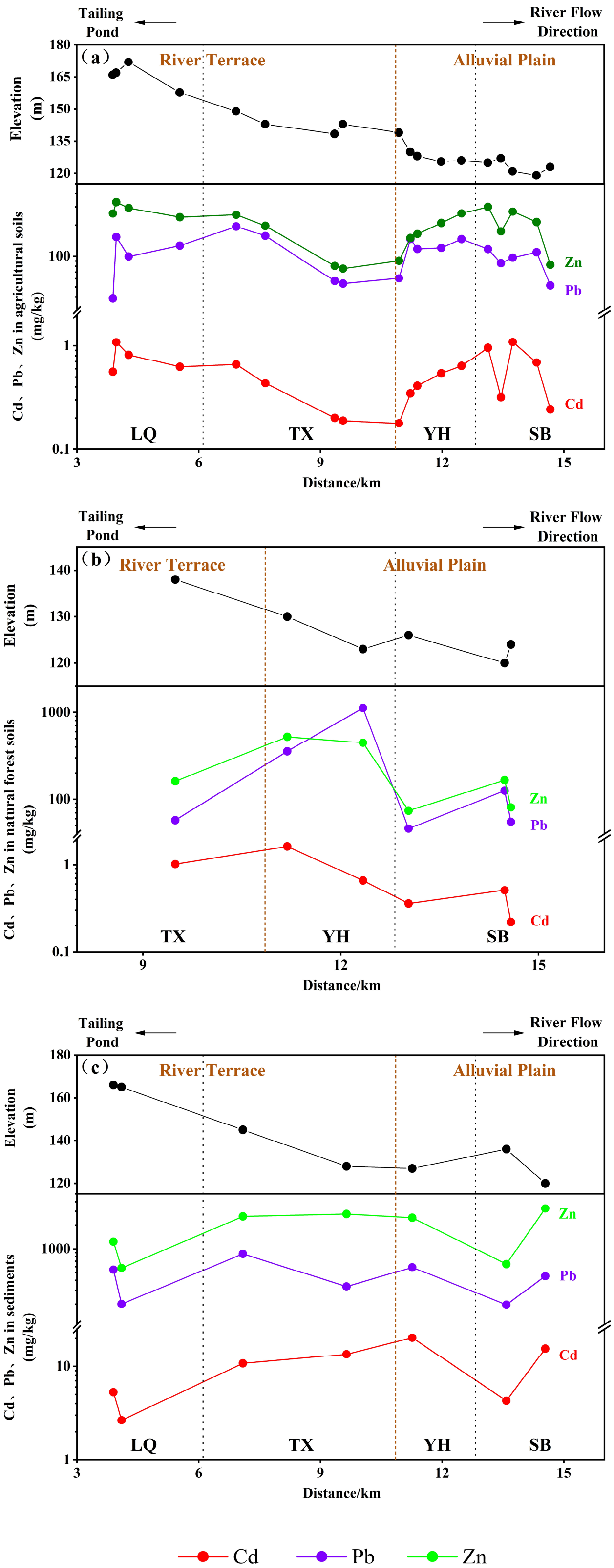

Figure 3. The spatial variation in Cd, Pb, and Zn content in different media and elevations in the study area, including agricultural soils (**a**), natural forest soils (**b**), and sediments (**c**). (Brown dash line: the boundary of topography; black dash line: the boundary of villages. LQ: Liangqiao Village, TX: Tangxin Village, YH: Yanghe Village, SB: Shangba Village).

Table 1. Statistical summaries of Cd, Pb, and Zn concentrations in rice grains from the study area (mg/kg).

	Min	Max	Mean	Median	SD	Coefficients Variation	MPL *	Exceedance Rate (%)
Cd	0.014	2.69	1.03	0.76	0.60	0.59	0.20	95.24%
Pb	0.02	0.39	0.12	0.08	0.08	0.72	0.40	0
Zn	15.60	23.90	18.99	18.64	1.75	0.09	50.00	0

Note(s): * MPL: The Chinese maximum permit levels (MPLs) for rice grains [38].

The concentration of Cd in rice grains and corresponding agricultural soils is shown in Figure 4. Except for FLS08, the concentration of Cd in rice grains gradually increases from the tailings pond to YH, reaches the maximum value near YH, and then gradually decreases. The variation characteristic of Pb in rice grains is similar to that of Cd. There is no obvious positive correlation between concentrations of PTEs in rice grains and in corresponding agricultural soils.

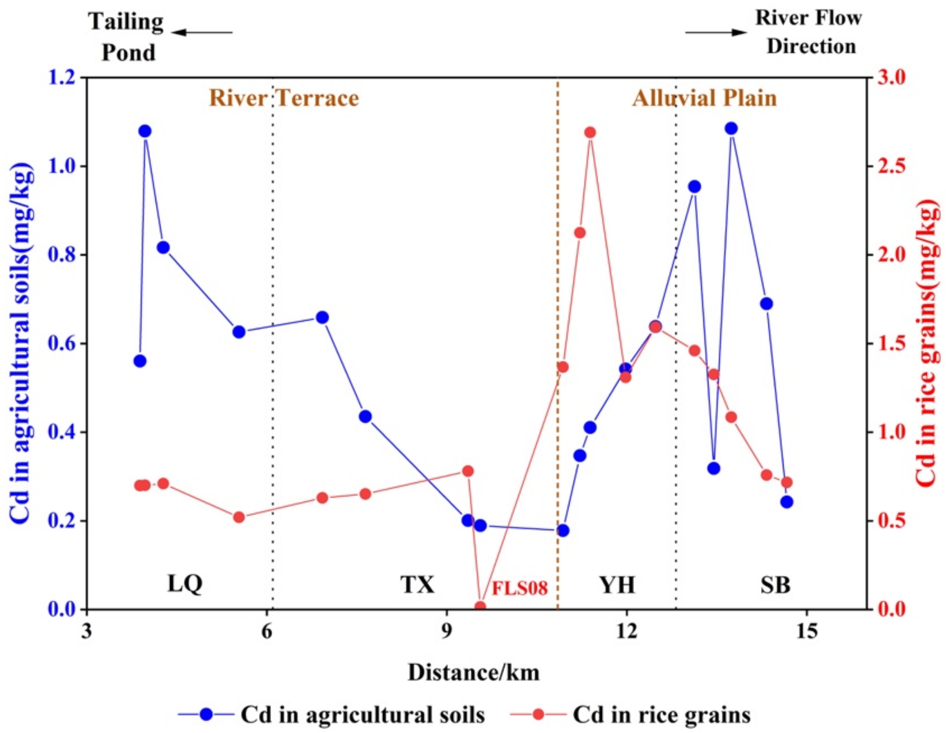

Figure 4. The spatial variation in Cd concentrations in rice grains and corresponding agricultural soils from the study area. (Brown dash line: the boundary of topography; black dash line: the boundary of village. LQ: Liangqiao Village, TX: Tangxin Village, YH: Yanghe Village, SB: Shangba Village).

4. Discussions

According to our results, although Cd, Pb, and Zn in sediments posed high ecological risk, Cd and Pb concentrations in soils were both lower than the risk intervention value, while in less than half of the soil, Zn exceeded the risk screening value, indicating there is no strict control area in Dabaoshan Mining area. However, the Cd concentration in 95.24% of rice grains exceeded the MPL, while concentrations of Pb and Zn in rice grain were found to be safe. These results demonstrate that, under a series of restoration efforts, the ecological risks posed by Pb and Zn have been gradually reduced and Cd contamination is the most severe in soils and rice grains around Dabaoshan Mine. Furthermore, the coefficients of variation in Cd, Pb, and Zn concentrations in rice grains (Table 1) revealed that Zn presented no significant spatial variation and Cd and Pb have similar variation characteristics. Therefore, in the following discussions, we focus on the factors affecting the Cd geochemical behavior in sediments, soil, and the soil–rice system.

4.1. Factors Affecting Cd Geochemical Behavior in Sediments

Cd concentrations in sediments increase from the tailings pond to the river terrace approximately 10 km away, then slightly decrease after Taiping River joins and flows into a small alluvial plain (Figure 3c). Cd is influenced by multiple geochemical processes during its migration and deposition in the river, including adsorption–desorption, hydraulic transport, and co−precipitation. Large amounts of AMD with low pH and high concentrations of PTE ions were produced by natural weathering and mining activities at Dabaoshan Mine, which changed the basic physicochemical properties of water and sediments in the Hengshi River and significantly affected the geochemical behavior of Cd in the river.

An important driving force for migration of PTEs in the river is hydraulic conditions, which are directly related to the elevation change of the river caused by topography. As the Hengshi River flows downstream along the valley, there is a significant decrease in river elevation, from 175 to 128 m. The river channel is narrow and river flow velocity is high in the section of the river terrace from LQ to TX. The riverbed gradually widens and the slope becomes very gentle in the alluvial plain section from YH to SB.

Cd in both dissolved and suspended forms originating from the tailings pond is not easily deposited in the river terrace and can accumulate in the alluvial plain, as supported by previous studies (Figure 3) [17,39,40].

The pH of water and the presence of secondary minerals in the river are also important factors controlling the migration of Cd in the upper Hengshi River. Figure 5 shows the changes in water pH under restoration efforts in the study area. In 2012, the water in Tielong tailings pond had an extremely low pH of approximately 2.39–2.81, primarily due to mine waste and runoff from the surrounding hills [41]. Since the Hengshi River flows through a very narrow valley with limited surface runoff, there is a lack of dilution in the river terrace. Cd in the river water migrated downstream in the form of divalent free ions or complexed compounds [26]. During the time of our sampling, the pH of the river water increased due to restoration measures, such as adding lime to the river, and the dilution effect of the Taiping River which is not contaminated by mining activities. However, the presence of various secondary minerals also plays a vital role in adsorption and migration of Cd in the river, which are susceptible to variation in pH. Schwertmannite is a hydroxy sulfate mineral that commonly exists in AMD, with a chemical formula of $Fe_8O_8(OH)_{8-2x}(SO_4)_x$ $1 \leq x \leq 1.75$ [42]. Schwertmannite exhibits a very high affinity for PTEs and has been observed in Hengshi River sediments [43,44]. Cd may co−precipitate and enter the solid phase during formation of schwertmannite and can be incorporated into the mineral lattice under very acidic conditions. However, as the pH of river water gradually increases, schwertmannite will gradually transform into more stable minerals such as goethite and ferrihydrite, causing Cd to be re−released predominantly in ionic form and absorbed in clay minerals [41,43].

4.2. Factors Affecting Cd Geochemical Behavior in Soil

The concentrations and distributions of Cd, Pb, and Zn in natural forest soils and agricultural soils show minimal differences (Figure 2). Cd, Pb, and Zn concentrations in agricultural soils are generally lower than those in natural forest soils within the same village, indicating that agricultural activities have not exacerbated Cd, Pb, and Zn pollution in the soils. The estimated contribution of fertilizer to soil Cd is only 1.21% based on input fluxes of Cd to agricultural soil near the Dabaoshan Mine [32]. Instead, crop harvesting may remove PTEs from soil. Therefore, PTEs in soils around Dabaoshan Mine are less influenced by anthropogenic activities, and AMD resulting from mining activities is likely the main source [45].

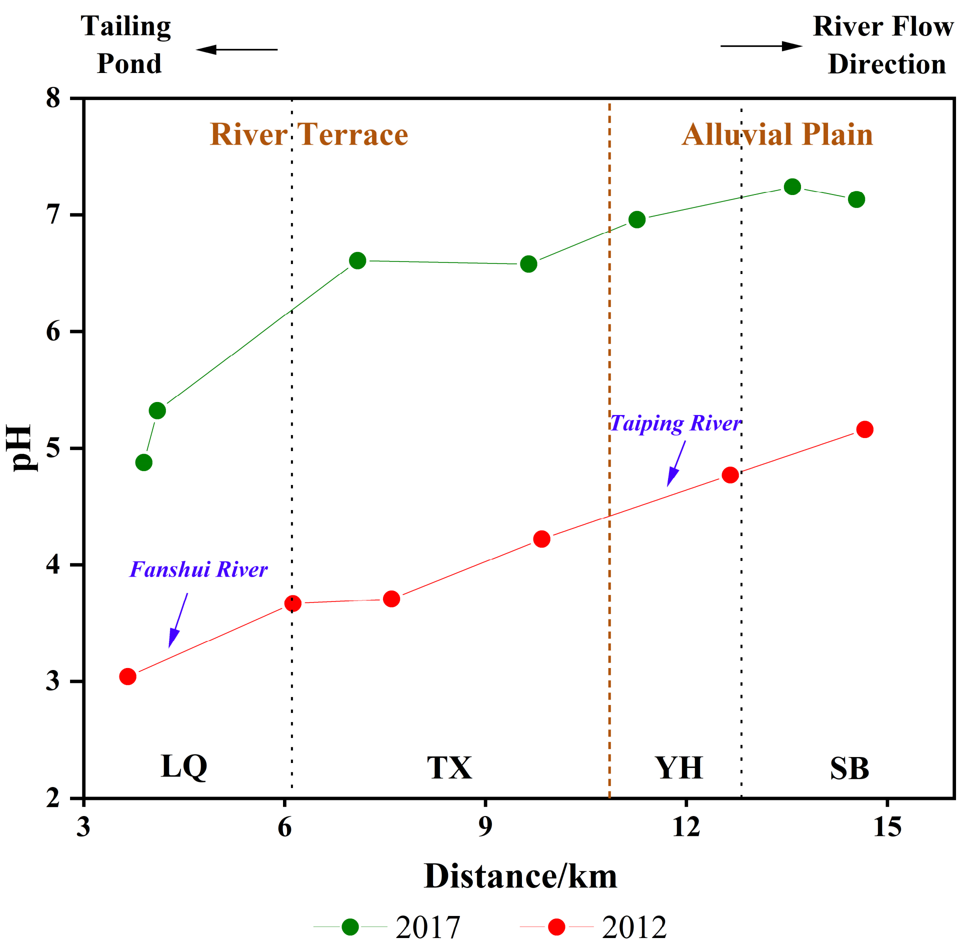

Figure 5. The spatial variation in river pH in 2012 [41] and in 2017 corresponding to sediments in the study area (brown dash line: the boundary of topography; black dash line: the boundary of village. LQ: Liangqiao Village, TX: Tangxin Village, YH: Yanghe Village, SB: Shangba Village).

Cd concentrations in soil showed the opposite trend to that in sediments (Figure 3a,b). The concentrations of Cd in soils are strongly affected by physicochemical properties of soil, including clay minerals and Fe−Mn oxides [46,47]. The Al_2O_3/SiO_2 ratio is an indicator of soil maturity, where higher values indicate finer soil texture and higher clay particle content [48]. The spatial variations in oxides, Al_2O_3/SiO_2, CEC, and pH in agricultural soils are shown in Figure 6.

In the river terrace, Al_2O_3/SiO_2 of agricultural soils shows a gradual decrease in the downstream direction, along with decreasing concentrations of oxides, CEC, and pH, which exhibit similar spatial distributions as those of Cd in agricultural soils (Figure 6). However, in the alluvial plain, Al_2O_3/SiO_2 of the agricultural soils gradually increases, while the concentration of TFe_2O_3 gradually decreases. The spatial patterns of these indexes in the agricultural soils do not align with spatial distributions of Cd concentrations, indicating that Cd concentrations in agricultural soils in the river terrace and alluvial plain may be affected by different factors.

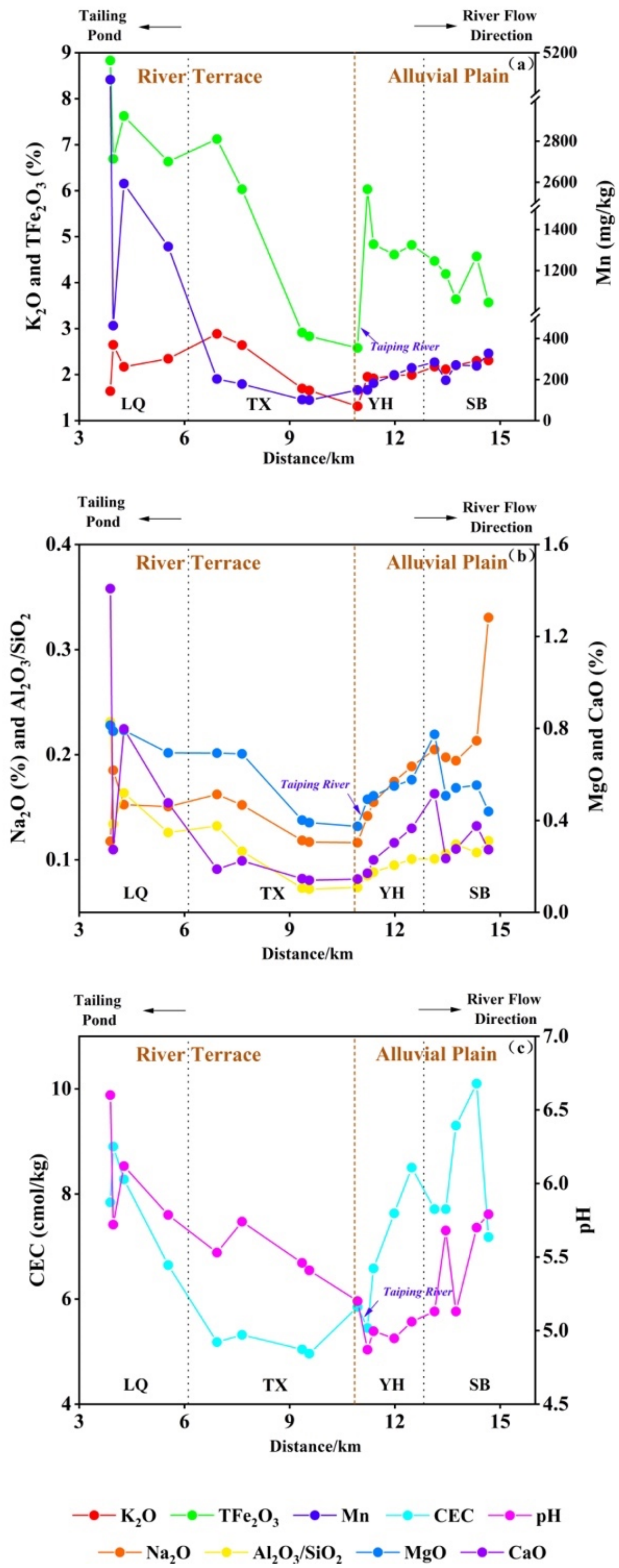

Figure 6. The spatial variation in oxides, Al_2O_3/SiO_2, CEC, and pH in agricultural soils from the study area ((**a**): K_2O, TFe_2O_3 and Mn; (**b**): Na_2O, Al_2O_3, MgO and CaO; (**c**): CEC and pH. Brown dash line: the boundary of topography; black dash line: the boundary of village. LQ: Liangqiao Village, TX: Tangxin Village, YH: Yanghe Village, SB: Shangba Village).

Random forest (RF) is a machine learning algorithm that can be used to assess the relative importance of soil physicochemical properties on Cd concentrations in soil [34]. In river terrace soils, TFe_2O_3, Mn, and CaO were identified as the most important factors affecting Cd concentration, with importance scores of 10.15%, 10.40%, and 9.72%, respectively (Figure 7). The steep slopes in the riverbed promote oxidation of the river water and the formation of Fe−Mn oxides. However, these conditions hinder sedimentation, resulting in colloids and oxides being transported downstream and deposited in more favorable locations [49]. The presence of CaO in the soil can reduce the solubility of Cd ions and decrease migration of Cd in the soil [50]. In the alluvial plain, the primary factors affecting Cd concentration in the agricultural soils are CaO, Al_2O_3/SiO_2, and Mn, with importance scores of 8.56%, 7.53%, and 7.22%, respectively. The score of TFe_2O_3 is only 1.90%, indicating that the influence of Fe oxides on Cd concentrations in the alluvial plain is relatively small. Decreased water flow velocity in the alluvial plain results in the preferential deposition of sand and silt, while fine−grained clay minerals migrate further, leading to a gradual increase in Al_2O_3/SiO_2 in agricultural soils, providing more adsorption sites for Cd [51]. The inflow of the Taiping River may be an important factor causing a gradual decrease in TFe_2O_3 concentration of the agricultural soils in the alluvial plain (Figure 6a). The Taiping River is not impacted by mining activities, and has the $Ca-HCO_3^-$ water quality type and a pH of about 7.09 [8]. The water pH of the upper Hengshi River gradually increases because of the dilution by the Taiping River (Figure 5). At the same time, schwertmannite minerals are metastable. When the water pH increases, SO_4^{2-} is gradually released from the schwertmannite mineral structure and is easily transformed into stable crystalline Fe oxide minerals (ferrihydrite, goethite, etc.) in the river, releasing a large amount of Cd [52,53]. This released Cd does not enter the structure of newly formed Fe oxide minerals and instead is adsorbed onto the surface of clay minerals in the form of ions [54].

4.3. Factors Influencing Migration of Cd in the Soil−Rice System

The ability of plants to absorb Cd from soil depends on bioavailability, which is influenced by various parameters such as pH, Eh, SOM, and Ca and Fe concentrations. The bioavailable concentration of Cd in soil is defined as the amount that is extractable by 0.01M $CaCl_2$, representing the most labile fraction [55]. The bioconcentration factor (BCF) represents the ability of rice grains to accumulate Cd from the agricultural soils, and is calculated using the following formula:

$$BCF_{Cd} = C_{grain}/C_{soil}$$

where C_{grain} is the Cd concentration in rice grains and C_{soil} is the Cd concentration in the corresponding agricultural soil.

The BCF for Cd in agricultural soil from the river terrace is lower than that from the alluvial plain and the degree of exceeding the MPL of Cd in rice grains increases from 238% to 573% along the river. The cumulative probability distribution curves for the proportion of $CaCl_2$−extracted Cd in soil and BCF_{Cd} in rice grains were fitted using a logistic function (Figure 8). Variations in BCF_{Cd} and proportion of $CaCl_2$−extracted Cd in soil are large, about 1–2 orders of magnitude, indicating significant spatial variations in the bioavailability of Cd in the study area. The mean values of BCF_{Cd} and proportion of $CaCl_2$−extracted Cd in the river terrace are lower than those in the alluvial plain, which indicates that Cd in agricultural soils posed greater potential ecological risk.

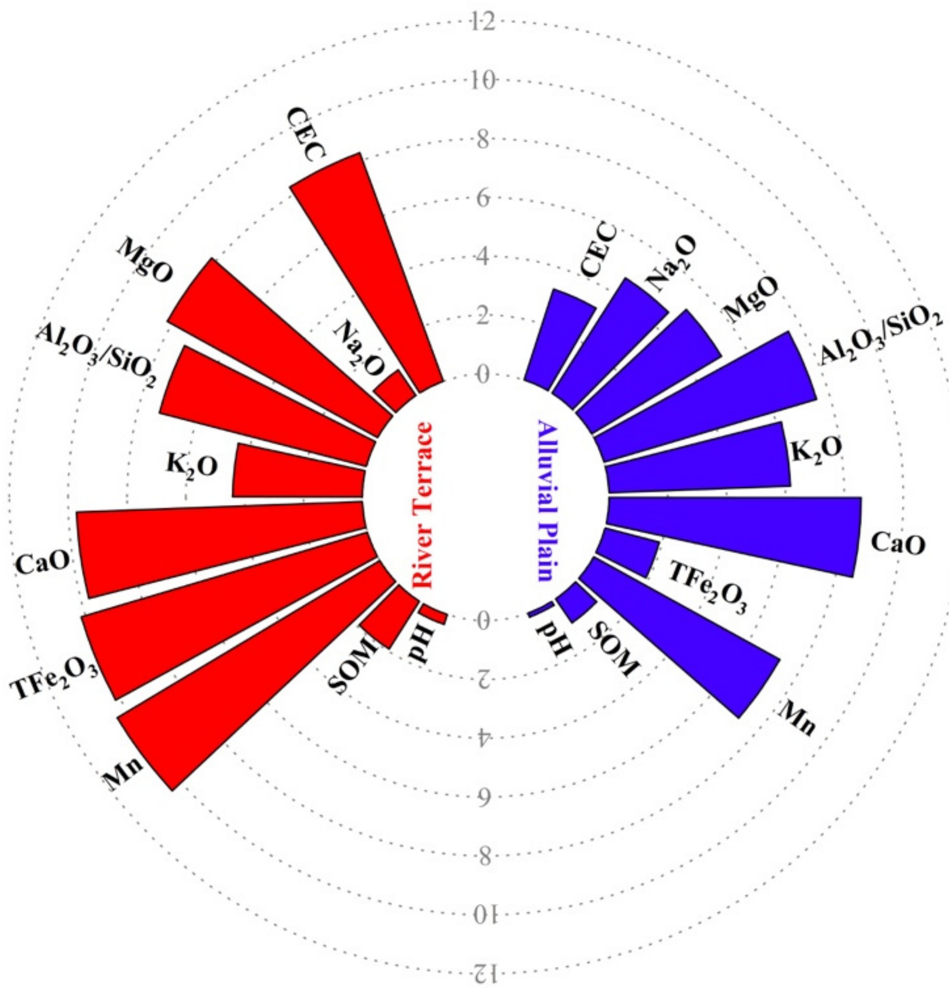

Figure 7. Importance scores of soil physicochemical properties influencing Cd concentration in soils from the river terrace and alluvial plain based on random forest (RF) analyses (unit: %).

Pearson correlation coefficients were calculated after logarithmic transformation (excluding pH) between BCF_{Cd} and soil physicochemical properties to better understand the factors affecting the bioavailability of Cd in agricultural soil (Table S6, Figure 9). In this diagram, the closer the dot to the center, the higher the negative correlation between each variable and Cd. In addition, the mazarine dot and azury dot represent significant correlations at $p < 0.01$ and $p < 0.05$, respectively. The BCF_{Cd} was found to have a significant negative correlation with Al_2O_3/SiO_2, K_2O, CaO, and MgO in agricultural soil. Soil clay minerals provide the main adsorption sites for Cd. The lower Al_2O_3/SiO_2 facilitates Cd desorption reactions, greatly increasing the bioavailability of Cd due to deposition sorting [41]. A decrease in clay mineral content also leads to lower CEC in soil, reducing exchangeable sites for PTE ions and increasing the activity of Cd [56].

An increase in the Ca^{2+} concentration in soil solution can reduce the solubility of Cd^{2+}, thereby reducing the bioavailability of Cd [57]. The high concentrations of Ca^{2+} and Mg^{2+} in the Taiping River result in precipitation of gypsum, which reduces the concentration of Ca^{2+} in soil solution [43].

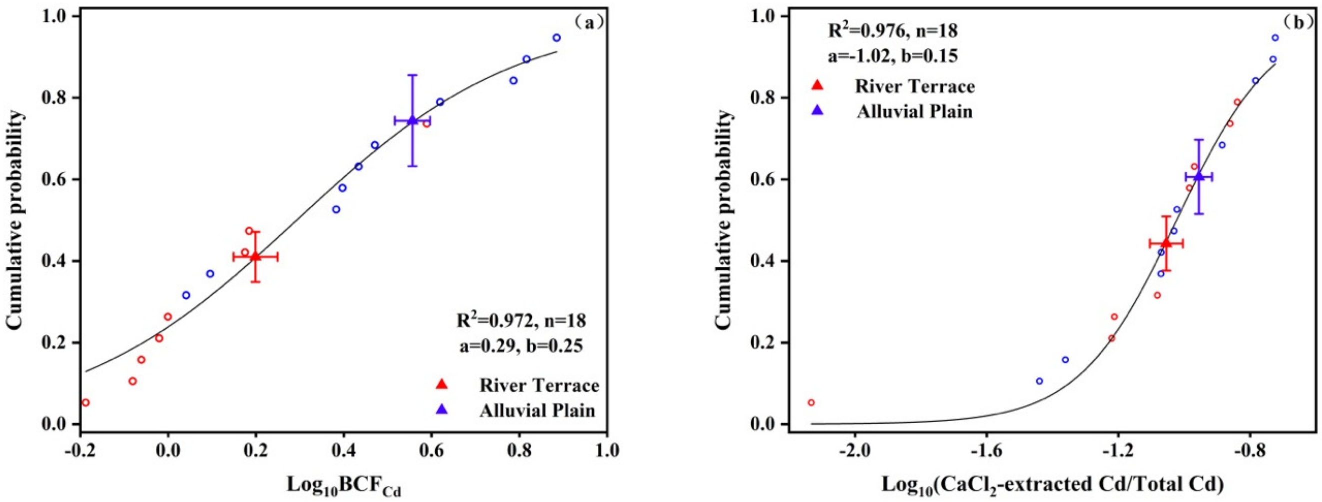

Figure 8. Cumulative probability distributions for: (**a**) BCF_{Cd} (bioconcentration factor), (**b**) proportion of $CaCl_2$−extracted Cd ($CaCl_2$−extracted Cd/total soil Cd). Red hollow dots: soil from river terrace; Blue hollow dots: soil from alluvial plain.

Fe−Mn oxide can promote adsorption of Cd^{2+} in soil solution, thereby reducing its bioavailability [58]. As previously described, Cd ions can co−precipitate with iron oxides such as schwertmannite and be re−released under phase transformations of these metastable minerals, increasing their activity. Meanwhile, reducing conditions caused by agricultural irrigation promote the reduction and dissolution of Fe−Mn oxides, enhancing the mobility and bioavailability of PTEs in the soil.

pH and SOM in the study area did not have a significant impact on the concentration and bioavailability of Cd in soil (Figures 7 and 8). On the one hand, pH can affect dynamic adsorption of Fe−Mn oxides on the surface of clay minerals. Ponthieu et al. [59] showed that when pH < 5.5 (such as on the YH–SB alluvial plain), Cd does not significantly adsorb onto amorphous iron oxides or goethite. Under very low pH conditions, negatively charged sites on the surface of clay minerals can be completely protonated, preventing binding of Cd to these sites [13]. On the other hand, binding of Cd ions to SOM is also controlled by pH. Previous research has shown that a pH change of at least 1–2 units is necessary to observe any effect of SOM on PTEs ions [60,61]. The relatively narrow pH range in the study area (ΔpH < 1.5) makes it challenging to accurately assess the impact of SOM on PTEs ions such as Cd.

Therefore, the decreases in clay mineral content due to deposition sorting and phase transformations of schwertmannite are indeed important factors that increase the bioavailability and ecological risk of Cd in alluvial plains. The resulting high Cd concentration in rice grains has led to an increase in the incidence of cancer.

4.4. Suggestions for Prevention and Control of PTE Contamination near Sulfide Mines

Properly managing sulfide mines with a science−based approach is crucial for the adequate treatment of environmental pollution and the effective prevention of ecological risk.

A series of restoration plans have been implemented in the areas affected by Dabaoshan Mine to reduce the impact of the mining activities on downstream ecosystems, including the construction of a sewage treatment plant [18], mud impoundment [17], and adding lime to the rivers near the mine [19]. Construction of the sewage treatment plant and mud impoundment has effectively improved the water quality of the Hengshi River in the dry season. However, the mud impoundment has gradually become full over time and AMD overflows during the rainy season, and the reactivation of PTEs in sediment has increased PTEs concentrations in the Hengshi River [30]. Although the addition of lime promotes the precipitation and adsorption of PTEs in river water, reducing their mobility [19], the increase in water pH may trigger the phase transformation of schwertmannite, releasing PTEs and increasing ecological risks.

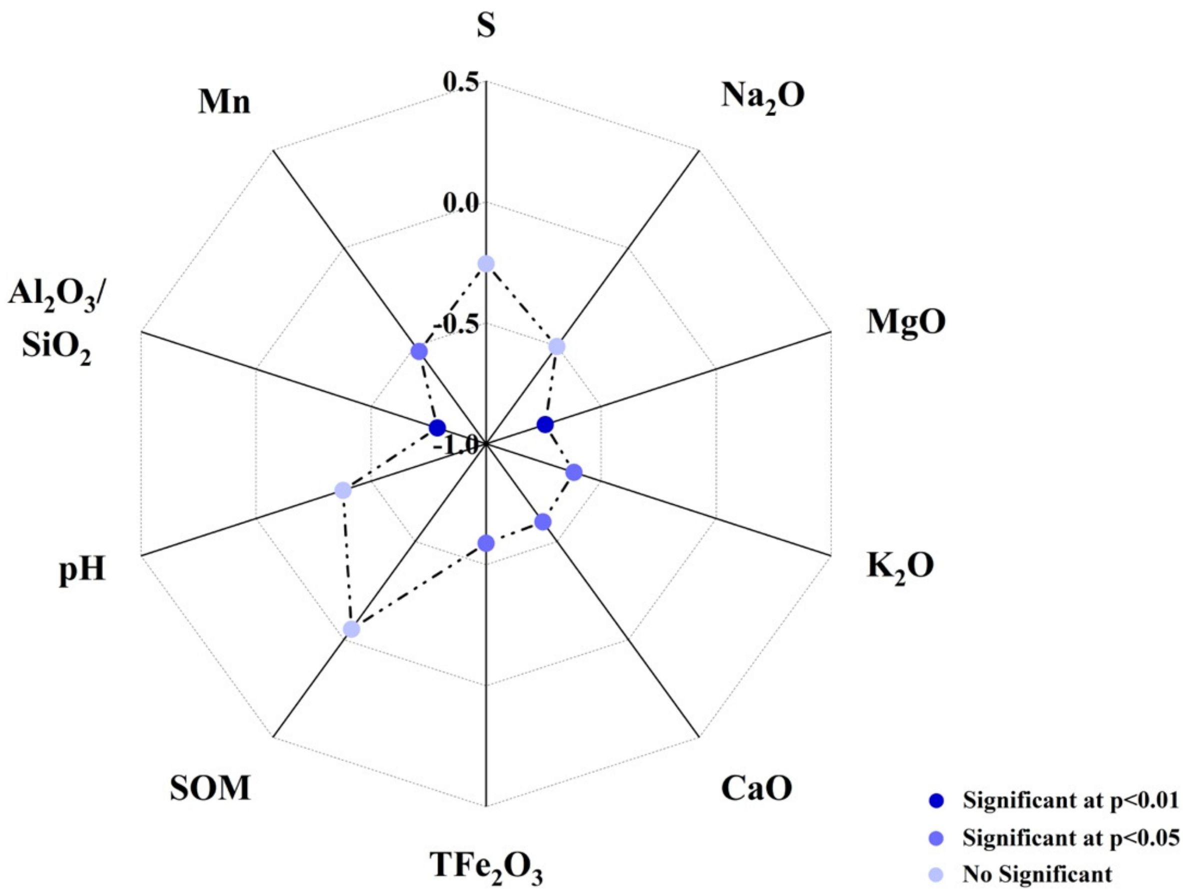

Figure 9. Correlation between the bioconcentration factor of Cd (BCF_{Cd}) and soil properties in agricultural soils from the study area.

Our study reveals significant differences in the concentrations and bioavailability of Cd in soils between river terraces and alluvial plains, along with their influencing factors. Therefore, classifying the surrounding environment of the sulfide mine according to topography can more precisely treat mining pollution, improve ecological risk prevention, and reduce PTE contamination of agricultural soil. In river terraces, it is recommended to reduce PTE loads through natural attenuation, relying on the environmental resilience, and to continuously monitor PTE concentrations in various environmental media [62]. In alluvial plains, plant restoration can be employed by introducing aquatic plants (such as reeds and cattails) in low−flow areas to stabilize sediment and absorb PTEs. Additionally, dredging can be used to remove contaminated sediment to avoid secondary release caused by changes in physiochemical conditions.

5. Conclusions

This study focused on the spatial distributions of Cd, Pb, and Zn in sediments and soils of Dabaoshan Mine, as well as the associated ecological risks after restoration efforts. The following conclusions were reached:

(1) Cd is the most prominent pollutant element, exhibiting significant enrichment and spatial heterogeneity in both soil and sediments, and higher accumulation levels in rice grains, in the Dabaoshan Mine area.

(2) The spatial distributions of Cd in sediments and soils are governed by topography, water velocity, channel width, change in physicochemical properties, and mineral composition of the upper Hengshi River.
(3) Areas posing the highest human health risks do not align with areas exhibiting the highest PTE concentrations in soil. Restoration efforts aimed at mitigating pollution may inadvertently alter the physicochemical properties of the river, leading to the transformation of schwertmannite, which affects the occurrence form of Cd and ultimately increases the potential ecological risk of Cd in soils within the alluvial plain.
(4) Although a series of restoration plans have been implemented, the Cd contamination problem in rice grains still persists. Taking topography into consideration when assessing the ecological risk of PTEs can enable effective pollution control and accurate prevention of potential ecological risks in the mining area.

Supplementary Materials: The following supporting information can be downloaded at: https://www.mdpi.com/article/10.3390/w15122223/s1. Figure S1 The geological map of study area (modified by National Geological Archive). Table S1. The Risk Screening Values (RSVs) and Risk Intervention Values (RIVs) for Cd, Pb and Zn in "Soil Environment Quality: Risk Control Standard for Soil Contamination of Agricultural Land" (GB15618-2018). Table S2. The Threshold Effect Level (TEL) and Probable Effect Level (PEL) of Cd, Pb, and Zn in Sediment Quality Guidelines (SQGs). Table S3. The concentrations of Cd, Pb, Zn, oxides and physicochemical properties of natural forest soil sampled in study area. Table S4. The concentrations of Rice grain and concentrations of Cd, Pb, Zn, oxides and physicochemical properties of corresponding agricultural soils sampled in study area. Table S5. The concentrations of Cd, Pb, Zn, oxides and physicochemical properties of sediments sampled in study area. Table S6. Pearson correlation coefficients between the bioconcentration factor of Cd (BCFCd) and soil properties in agricultural soils from the study area.

Author Contributions: W.S.: Methodology, Data curation, Formal analysis, Writing—original draft; Q.H.: Conceptualization, Methodology, Funding acquisition, Writing—Review and Editing; Z.Y.: Project administration, Supervision, Writing—Review and Editing; T.Y.: Resources. All authors have read and agreed to the published version of the manuscript.

Funding: This research was financially supported by the Natural Science Foundation of China (Project No. 41773019), the National Key R&D Program of China (Project No. 2017YFD0800304) and Guangdong Geological Exploration and Urban Geology Project (Grant No. 2023-25).

Institutional Review Board Statement: Not needed or available.

Informed Consent Statement: Not available or needed for this study.

Data Availability Statement: Data used in this study are available from the first authors upon reasonable request.

Conflicts of Interest: The authors declare no conflict of interest.

References

1. Mahar, A.; Wang, P.; Ali, A.; Awasthi, M.K.; Lahori, A.H.; Wang, Q.; Li, R.; Zhang, Z. Challenges and opportunities in the phytoremediation of heavy metals contaminated soils: A review. *Ecotoxicol. Environ. Saf.* **2016**, *126*, 111–121. [CrossRef] [PubMed]
2. Martin, C.W. Trace metal concentrations along tributary streams of historically mined areas, Lower Lahn and Dill River basins, central Germany. *CATENA* **2018**, *174*, 174–183. [CrossRef]
3. Damian, G.E.; Micle, V.; Sur, I.M.; Băbău, A.M.C. From Environmental Ethics to Sustainable Decision-Making: Assessment of Potential Ecological Risk in Soils Around Abandoned Mining Areas-Case Study "Larga de Sus mine" (Romania). *J. Agric. Environ. Ethic* **2019**, *32*, 27–49. [CrossRef]
4. Huang, S.; Li, Q.; Yang, Y.; Yuan, C.; You, P. Risk Assessment of Heavy Metals in Soils of a Lead-Zinc Mining Area in Hunan Province (China). *J. Chem. Chem. Eng.* **2017**, *66*, 173–178. [CrossRef]
5. Pearson, J.; Ipsen, J.; Sutherland, S.; Wegerson, K.; Onello, E. Risks and costs to human health of sulfide-ore mining near the Boundary Waters Canoe Area Wilderness. *Hum. Ecol. Risk Assess. Int. J.* **2019**, *26*, 1329–1340. [CrossRef]
6. Pietro, M.; Gerardo, B.; Giulia, S.; Monica, S.; Valentina, M.; Christian, M.; Paola, S. Geoheritage Values and Environmental Issues of Derelict Mines: Examples from the Sulfide Mines of Gromolo and Petronio Valley (Eastern Liguria, Italy). *Minerals* **2018**, *8*, 229.
7. Yang, S.; Ge, W.-Y.; Chen, H.-H.; Xu, W.-L. Investigation of soil and groundwater environment in urban area during post-industrial era: A case study of brownfield in Zhenjiang, Jiangsu Province, China. *China Geol.* **2019**, *2*, 501–511. [CrossRef]

8. Zhao, H.; Xia, B.; Qin, J.; Zhang, J. Hydrogeochemical and mineralogical characteristics related to heavy metal attenuation in a stream polluted by acid mine drainage: A case study in Dabaoshan Mine, China. *J. Environ. Sci.* **2012**, *24*, 979–989. [CrossRef]
9. Wang, M.; Song, H.; Chen, W.-Q.; Lu, C.; Hu, Q.; Ren, Z.; Yang, Y.; Xu, Y.; Zhong, A.; Ling, W. Cancer mortality in a Chinese population surrounding a multi-metal sulphide mine in Guangdong province: An ecologic study. *BMC Public Health* **2011**, *11*, 319. [CrossRef]
10. Gao, K.; Jiang, M.; Guo, C.; Zeng, Y.; Fan, C.; Zhang, J.; Reinfelder, J.; Huang, W.; Lu, G.; Dang, Z. Reductive dissolution of jarosite by a sulfate reducing bacterial community: Secondary mineralization and microflora development. *Sci. Total Environ.* **2019**, *690*, 1100–1109. [CrossRef]
11. Zhou, J.-M.; Dang, Z.; Cai, M.-F.; Liu, C.-Q. Soil Heavy Metal Pollution around the Dabaoshan Mine, Guangdong Province, China. *Pedosphere* **2007**, *17*, 588–594. [CrossRef]
12. Chan, W.S.; Routh, J.; Luo, C.; Dario, M.; Miao, Y.; Luo, D.; Wei, L. Metal accumulations in aquatic organisms and health risks in an acid mine-affected site in South China. *Environ. Geochem. Health* **2021**, *43*, 4415–4440. [CrossRef]
13. Li, Y.-T.; Becquer, T.; Dai, J.; Quantin, C.; Benedetti, M.F. Ion activity and distribution of heavy metals in acid mine drainage polluted subtropical soils. *Environ. Pollut.* **2009**, *157*, 1249–1257. [CrossRef] [PubMed]
14. Qu, L.; Xie, Y.; Lu, G.; Yang, C.; Zhou, J.; Yi, X.; Dang, Z. Distribution, fractionation, and contamination assessment of heavy metals in paddy soil related to acid mine drainage. *Paddy Water Environ.* **2017**, *15*, 553–562. [CrossRef]
15. Zhuang, P.; McBride, M.B.; Xia, H.; Li, N.; Li, Z. Health risk from heavy metals via consumption of food crops in the vicinity of Dabaoshan mine, South China. *Sci. Total Environ.* **2009**, *407*, 1551–1561. [CrossRef] [PubMed]
16. Liao, J.; Wen, Z.; Ru, X.; Chen, J.; Wu, H.; Wei, C. Distribution and migration of heavy metals in soil and crops affected by acid mine drainage: Public health implications in Guangdong Province, China. *Ecotoxicol. Environ. Saf.* **2016**, *124*, 460–469. [CrossRef]
17. Chen, M.; Lu, G.; Wu, J.; Yang, C.; Niu, X.; Tao, X.; Shi, Z.; Yi, X.; Dang, Z. Migration and fate of metallic elements in a waste mud impoundment and affected river downstream: A case study in Dabaoshan Mine, South China. *Ecotoxicol. Environ. Saf.* **2018**, *164*, 474–483. [CrossRef]
18. He, Q. *The Migration of Heavy Metals in the Surface Runoff of Dabaoshan Mining Area*; South China University of Technology: Guangzhou, China, 2011.
19. Wei, L.; Liu, Y.; Cai, D.; Li, F.; Luo, D.; Li, C.; Xu, G.; Xiao, T.; Wu, Q.; He, H.; et al. River morphology redistributes potentially toxic elements in acid mine drainage-impacted river sediments: Evidence, causes, and implications. *Catena* **2022**, *214*, 106183. [CrossRef]
20. Hou, D.; O'Connor, D.; Nathanail, P.; Tian, L.; Ma, Y. Integrated GIS and multivariate statistical analysis for regional scale assessment of heavy metal soil contamination: A critical review. *Environ. Pollut.* **2017**, *231*, 1188–1200. [CrossRef]
21. Zhao, H.; Xia, B.; Fan, C.; Zhao, P.; Shen, S. Human health risk from soil heavy metal contamination under different land uses near Dabaoshan Mine, Southern China. *Sci. Total Environ.* **2012**, *417–418*, 45–54. [CrossRef]
22. Su, W.; Xu, Y.; Fan, S.; Fu, S. The distribution regularity and accumulation risk of heavy metals in water and soil along the Hengshi River in the Dabaoshan mining area, Guangdong Province. *Geol. Bull. China* **2014**, *33*, 1231–1238.
23. Huang, J.; Qin, M.; Ma, W.; Yu, J.; Peng, X.; Yang, L. Characteristics analysis and ecological risk assessment of heavy metals contamination in suspend solids in a river affected by acid mine drainage. *Environ. Chem.* **2016**, *35*, 2315–2326.
24. Shu, X.-H.; Zhang, Q.; Lu, G.-N.; Yi, X.-Y.; Dang, Z. Pollution characteristics and assessment of sulfide tailings from the Dabaoshan Mine, China. *Int. Biodeterior. Biodegrad.* **2018**, *128*, 122–128. [CrossRef]
25. Zhuang, P.; Zou, B.; Li, N.Y.; Li, Z.A. Heavy metal contamination in soils and food crops around Dabaoshan mine in Guangdong, China: Implication for human health. *Environ. Geochem. Health* **2009**, *31*, 707–715. [CrossRef] [PubMed]
26. Yang, W.-J.; Ding, K.-B.; Zhang, P.; Qiu, H.; Cloquet, C.; Wen, H.-J.; Morel, J.-L.; Qiu, R.-L.; Tang, Y.-T. Cadmium stable isotope variation in a mountain area impacted by acid mine drainage. *Sci. Total Environ.* **2019**, *646*, 696–703. [CrossRef]
27. Wang, Y.; Dong, R.; Zhou, Y.; Luo, X. Characteristics of groundwater discharge to river and related heavy metal transportation in a mountain mining area of Dabaoshan, Southern China. *Sci. Total Environ.* **2019**, *679*, 346–358. [CrossRef]
28. Liao, J.; Ru, X.; Xie, B.; Zhang, W.; Wu, H.; Wu, C.; Wei, C. Multi-phase distribution and comprehensive ecological risk assessment of heavy metal pollutants in a river affected by acid mine drainage. *Ecotoxicol. Environ. Saf.* **2017**, *141*, 75–84. [CrossRef] [PubMed]
29. Ye, L.; Liu, T.; Yang, Y.; Gao, W.; Pan, Z.; Bao, T. Petrogenesis of bismuth minerals in the Dabaoshan Pb–Zn polymetallic massive sulfide deposit, northern Guangdong Province, China. *J. Asian Earth Sci.* **2014**, *82*, 1–9. [CrossRef]
30. Luo, C.; Routh, J.; Dario, M.; Sarkar, S.; Wei, L.; Luo, D.; Liu, Y. Distribution and mobilization of heavy metals at an acid mine drainage affected region in South China, a post-remediation study. *Sci. Total Environ.* **2020**, *724*, 138122. [CrossRef]
31. Chen, A.; Lin, C.; Lu, W.; Wu, Y.; Ma, Y.; Li, J.; Zhu, L. Well water contaminated by acidic mine water from the Dabaoshan Mine, South China: Chemistry and toxicity. *Chemosphere* **2008**, *70*, 248–255. [CrossRef]
32. Chen, Q.; Ma, M.; You, Y.; Yang, D. Cadmium Input Flux in Farmland Soil Near the Dabaoshan Mining Area of Guangdong Province. *Geol. Miner. Resour. South China* **2020**, *36*, 147–152.
33. Bussan, D.; Harris, A.; Douvris, C. Monitoring of selected trace elements in sediments of heavily industrialized areas in Calcasieu Parish, Louisiana, United States by inductively coupled plasma-optical emission spectroscopy (ICP-OES). *Microchem. J.* **2019**, *144*, 51–55. [CrossRef]
34. Breiman, L. Random forests. *Mach. Learn.* **2001**, *45*, 5–32. [CrossRef]

35. Li, C.; Zhang, C.; Yu, T.; Ma, X.; Yang, Y.; Liu, X.; Hou, Q.; Li, B.; Lin, K.; Yang, Z.; et al. Identification of soil parent materials in naturally high background areas based on machine learning. *Sci. Total Environ.* **2023**, *875*, 162684. [CrossRef]
36. *GB 15618-2018*; Soil Environment Quality-Risk Control Standard for Soil Contamination of Agricultural Land. Standard Press of China: Beijing, China, 2018. (In Chinese)
37. Yu, Z.; Liu, E.; Lin, Q.; Zhang, E.; Yang, F.; Wei, C.; Shen, J. Comprehensive assessment of heavy metal pollution and ecological risk in lake sediment by combining total concentration and chemical partitioning. *Environ. Pollut.* **2020**, *269*, 116212. [CrossRef]
38. *NY 861-2004*; Limits of Eight Elements in Cereals, Legume, Tubes and Its Products. Standard Press of China: Beijing, China, 2005.
39. Zhou, X.; Xia, B. Defining and modeling the soil geochemical background of heavy metals from the Hengshi River watershed (southern China): Integrating EDA, stochastic simulation and magnetic parameters. *J. Hazard. Mater.* **2010**, *180*, 542–551. [CrossRef] [PubMed]
40. Mueller, E.R.; Grams, P.E.; Schmidt, J.C.; Hazel, J.E.; Alexander, J.S.; Kaplinski, M. The influence of controlled floods on fine sediment storage in debris fan-affected canyons of the Colorado River basin. *Geomorphology* **2014**, *226*, 65–75. [CrossRef]
41. Chen, M.; Lu, G.; Guo, C.; Yang, C.; Wu, J.; Huang, W.; Yee, N.; Dang, Z. Sulfate migration in a river affected by acid mine drainage from the Dabaoshan mining area, South China. *Chemosphere* **2015**, *119*, 734–743. [CrossRef]
42. Regenspurg, S.; Brand, A.; Peiffer, S. Formation and stability of schwertmannite in acidic mining lakes. *Geochim. Cosmochim. Acta* **2004**, *68*, 1185–1197. [CrossRef]
43. Xie, Y.; Lu, G.; Yang, C.; Qu, L.; Chen, M.; Guo, C.; Dang, Z. Mineralogical characteristics of sediments and heavy metal mobilization along a river watershed affected by acid mine drainage. *PLoS ONE* **2018**, *13*, e0190010. [CrossRef]
44. Chen, M.; Lu, G.; Wu, J.; Sun, J.; Yang, C.; Xie, Y.; Wang, K.; Deng, F.; Yi, X.; Dang, Z. Acidity and metallic elements release from AMD-affected river sediments: Effect of AMD standstill and dilution. *Environ. Res.* **2020**, *186*, 109490. [CrossRef]
45. Liu, Y.; Gao, T.; Xia, Y.; Wang, Z.; Liu, C.; Li, S.; Wu, Q.; Qi, M.; Lv, Y. Using Zn isotopes to trace Zn sources and migration pathways in paddy soils around mining area. *Environ. Pollut.* **2020**, *267*, 115616. [CrossRef] [PubMed]
46. Yu, X.; Lu, S. Micrometer-scale internal structure and element distribution of Fe-Mn nodules in Quaternary red earth of Eastern China. *J. Soils Sediments* **2015**, *16*, 621–633. [CrossRef]
47. Wu, W.; Qu, S.; Nel, W.; Ji, J. The impact of natural weathering and mining on heavy metal accumulation in the karst areas of the Pearl River Basin, China. *Sci. Total Environ.* **2020**, *734*, 139480. [CrossRef] [PubMed]
48. Makabe, S.; Kakuda, K.-I.; Sasaki, Y.; Ando, T.; Ando, H. Relationship between mineral composition or soil texture and available silicon in alluvial paddy soils on the Shounai Plain, Japan. *Soil Sci. Plant Nutr.* **2009**, *55*, 300–308. [CrossRef]
49. Ma, Y.; Lu, W.; Lin, C. Downstream patterns of bed sediment-borne metals, minerals and organic matter in a stream system receiving acidic mine effluent: A preliminary study. *J. Geochem. Explor.* **2011**, *110*, 98–106. [CrossRef]
50. Guo, C.; Wen, Y.; Yang, Z.; Li, W.; Guan, D.; Ji, J. Factor controlling the bioavailability of soil cadmium in typical karst areas with high geogenic background. *J. Nanjing Univ. Nat. Sci.* **2019**, *55*, 678–687.
51. Guo, L.; Su, N.; Townend, I.; Wang, Z.B.; Zhu, C.; Wang, X.; Zhang, Y.; He, Q. From the headwater to the delta: A synthesis of the basin-scale sediment load regime in the Changjiang River. *Earth-Sci. Rev.* **2019**, *197*, 102900. [CrossRef]
52. Paikaray, S.; Schröder, C.; Peiffer, S. Schwertmannite stability in anoxic Fe(II)-rich aqueous solution. *Geochim. Cosmochim. Acta* **2017**, *217*, 292–305. [CrossRef]
53. Cruz-Hernandez, P.; Carrero, S.; Pérez-López, R.; Fernandez-Martinez, A.; Lindsay, M.; Dejoie, C.; Nieto, J.M. Influence of As(V) on precipitation and transformation of schwertmannite in acid mine drainage-impacted waters. *Eur. J. Miner.* **2019**, *31*, 237–245. [CrossRef]
54. Acero, P.; Ayora, C.; Torrentó, C.; Nieto, J.-M. The behavior of trace elements during schwertmannite precipitation and subsequent transformation into goethite and jarosite. *Geochim. Cosmochim. Acta* **2006**, *70*, 4130–4139. [CrossRef]
55. Houba, V.J.G.; Temminghoff, E.J.M.; Gaikhorst, G.A. Soil analysis procedures using 0.01 M calcium chloride as extraction reagent. *Commun. Soil Sci. Plant Anal.* **2000**, *31*, 1299–1396. [CrossRef]
56. Razzaghi, F.; Arthur, E.; Moosavi, A.A. Evaluating models to estimate cation exchange capacity of calcareous soils. *Geoderma* **2021**, *400*, 115221. [CrossRef]
57. Gray, C.W.; Mclaren, R.G.; Roberts, A.H.C.; Condron, L.M. Solubility, sorption and desorption of native and added cadmium in relation to properties of soils in New Zealand. *Eur. J. Soil Sci.* **1999**, *50*, 127–137. [CrossRef]
58. Wang, J.; Wang, P.-M.; Gu, Y.; Kopittke, P.M.; Zhao, F.-J.; Wang, P. Iron–Manganese (Oxyhydro)oxides, Rather than Oxidation of Sulfides, Determine Mobilization of Cd during Soil Drainage in Paddy Soil Systems. *Environ. Sci. Technol.* **2019**, *53*, 2500–2508. [CrossRef] [PubMed]
59. Ponthieu, M.; Juillot, F.; Hiemstra, T.; van Riemsdijk, W.; Benedetti, M. Metal ion binding to iron oxides. *Geochim. Cosmochim. Acta* **2006**, *70*, 2679–2698. [CrossRef]
60. Kinniburgh, D.G.; van Riemsdijk, W.H.; Koopal, L.K.; Borkovec, M.; Benedetti, M.F.; Avena, M.J. Ion binding to natural organic matter: Competition, heterogeneity, stoichiometry and thermodynamic consistency. *Colloids Surf. A* **1999**, *151*, 147–166. [CrossRef]

61. Milne, C.J.; Kinniburgh, D.G.; van Riemsdijk, W.H.; Tipping, E. Generic NICA−Donnan Model Parameters for Metal-Ion Binding by Humic Substances. *Environ. Sci. Technol.* **2003**, *37*, 958–971. [CrossRef]
62. Dore, E.; Fancello, D.; Rigonat, N.; Medas, D.; Cidu, R.; Da Pelo, S.; Frau, F.; Lattanzi, P.; Marras, P.A.; Meneghini, C.; et al. Natural attenuation can lead to environmental resilience in mine environment. *Appl. Geochem.* **2020**, *117*, 104597. [CrossRef]